PHYSICAL REVIEW A **92**, 013406 (2015)

Spectrum of quasistable states in a strong infrared field

Changchun Zhong* and F. Robicheaux†

Department of Physics and Astronomy, Purdue University, West Lafayette, Indiana 47907, USA

(Received 18 May 2015; published 13 July 2015)

The quasistability of highly exicited H and He atoms in a strong infrared (IR) field is studied based on three-dimensional quantum calculations. The spectra of atoms that survive the IR field show a series of IR-frequency-modulated peaks that extend from deeply bound states all the way to the ionization threshold and above. The atoms that survive mainly consist of highly excited Rydberg states, even after hundreds of the intense IR cycles. Also, they tend to have initial energies that allow emission or absorption of an integer number of IR photons to reach these quasistable states. Peaks above the ionization threshold in the survival spectra indicate the existence of multiphoton-assisted recombination in the intense IR field.

DOI: 10.1103/PhysRevA.92.013406 PACS number(s): 32.80.Rm, 32.80.Wr

I. INTRODUCTION

Quasistable states of Li atoms in a strong microwave field have recently been discussed in Refs. [1–5]. Arakelyan *et al.* [3] showed that when laser-excited atoms of Li were exposed to an intense microwave pulse, ∼10% of the atoms were found in Rydberg states subsequent to the pulse, even if the microwave was far more intense than that required for static-field ionization. A similar phenomenon of atoms in a strong laser pulse has been predicted and extensively discussed for the past half century [6–8]. Various mechanisms for strong-field stabilization of atoms have been proposed [9–12], and some related experimental papers can be found in Refs. [13–15].

Considering the existence of quasistable states of atoms in the presence of a strong microwave field, it is possible to study them spectrally. In the microwave experiment of Refs. [2,3], Arakelyan *et al.* measured the optical spectra of Li atoms that survive the strong microwave field. They found a periodic train of peaks separated by the microwave frequency. The experimental observations suggest that Li atoms survive the intense microwave field in quasistable states, where the Rydberg electron stays in a weakly bound orbit infrequently visiting the Li core. Interestingly, the spectrum also revealed peaks above the ionization threshold, which is explained by multiphoton-assisted recombination [4,5]. Those electrons excited to the continuum are able to stimulatedly emit a certain number of microwave photons, thus causing the recombination of ions and electrons [5].

Since quasistable states can also form in an intense laser field [6–8], one natural thing to do is to detect them spectrally. In this paper, we spectrally probe the quasistable states of H and He atoms in the presence of an intense IR field by numerically solving the three-dimensional (3D) time-dependent Schrödinger equation. In order to simulate a prospective experiment, the IR laser is smoothly turned on and off in our calculation, and a weak UV laser is used to prepare atoms at the desired states, as shown in Fig. 1(a). After the IR laser is turned off, we compute the probability of atoms in excited, bound states. The survival spectra show a periodic train of peaks separated by the IR frequency extending from deeply bound states to the ionization threshold and above. To get more information about the bound electrons, we also calculate the survival population as a function of principal quantum number of the electron after the IR field is turned off. The results show that the majority of the population is concentrated in high-lying states. Our analysis not only indicates the existence of multiphoton-assisted recombination in a strong IR field but also reveals that the atoms in IR fields, similar to the case in microwave fields, derive the quasistability from the time electrons spend away from the nucleus. In the sections that follow, we introduce the numerical approach that we use, present the results and analysis, compare them to our expectations, and comment on their implications.

We use atomic units (a.u.) except where explicitly stated otherwise.

II. THEORY AND METHOD

Similar to the recent experiment of Li in a microwave field [3], we assume all atoms are in the ground state at the beginning, then a weak UV laser is turned on to bring atoms to the desired states through one-photon absorption, while the IR field is on all the time. In the numerical simulation, we treat the UV laser as a source term since it is weak. After the UV laser is off, the source term stops providing electrons to the near-threshold energy region. The IR field keeps interacting with the atoms until it is smoothly turned off. Figure 1 shows a schematic picture of the time evolution of atoms, with the short arrows in Fig. 1(b) denoting the IR laser-induced multiphoton transitions. The wavelength of the IR field is fixed at $\lambda = 1000$ nm, which corresponds to frequency $\omega \sim 0.0455$ a.u. The intense IR field is treated in a nonperturbative manner. In order to study the influence of the IR field strength on the quasistable states of atoms, we use six different IR intensities, which are I, $4I$, $9I$, $16I$, $25I$, $36I$, with $I = 2.66 \times 10^{11}$ W/cm^2. These IR intensities are weak in the sense of affecting the ground states of H and He atoms, while strong in the sense of interacting with their excited states.

The dynamics is governed by the following time-dependent Schrödinger equation:

$$i\frac{\partial \Psi(\vec{r},t)}{\partial t} = H\Psi(\vec{r},t), \tag{1}$$

*zchangch@purdue.edu
†robichf@purdue.edu

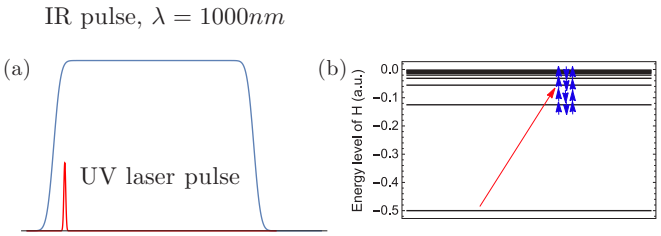

FIG. 1. (Color online) (a) The timing envelope for the UV laser and IR field used in our simulation. We choose the duration of the UV laser (four IR cycles) in a way that is short on the scale of the IR duration and long on the scale of IR laser cycles. The duration of the IR is about 1.6×10^4 a.u. (b) Each black line corresponds to an energy level of the H atom. The red arrow shows the electron being brought to the desired state by an UV laser. Then the electron (blue arrow) continues evolving in the presence of the IR field plus atomic potential.

where the wave function and Hamiltonian can be written in the form $\Psi(\vec{r},t) = \Psi_g(\vec{r},t) + \Psi_e(\vec{r},t)$, and $H = H_0 + H_{\rm UV} + H_{\rm IR}$. $\Psi_g(\vec{r},t)$ is the ground-state wave function and $\Psi_e(\vec{r},t)$ is the wave function of the electron after it has absorbed one UV photon. In the simulation, the IR field is treated nonperturbatively while the UV laser is treated using first-order time-dependent perturbation approximation. Noticing $i\partial\Psi_g(\vec{r},t)/\partial t = H_0\Psi_g(\vec{r},t)$, Eq. (1) can be written as

$$i\frac{\partial\Psi_e(\vec{r},t)}{\partial t} - \tilde{H}\Psi_e(\vec{r},t) = S(\vec{r},t) = H_{\rm UV}\Psi_g(\vec{r},t). \quad (2)$$

$S(\vec{r},t) = F_{\rm UV}(t)z\Psi_g(\vec{r})\exp[-i(E_g+\omega_{\rm UV})t]$, which acts as a source of amplitude for $\Psi_e(\vec{r},t)$. The UV laser in the source takes a Gaussian envelope, $F_{\rm UV}(t) \propto \exp(-t^2/2t_w^2)$ and t_w is chosen to make sure it lasts 4 IR periods in time (the duration controls the peak width in the energy domain). $\Psi_e(\vec{r},t)$ is initially zero everywhere before the UV laser is on. $\tilde{H} = H_0 + H_{\rm IR}$, which reads

$$\tilde{H} = -\tfrac{1}{2}\nabla^2 + V(\vec{r}) - F_{\rm IR}(t)z. \quad (3)$$

The third term in Eq. (3) is the interaction (dipole approximation is used) between the atom and the IR field (linearly polarized). The IR field strength is

$$F_{\rm IR}(t) = F_{\max}\cos(\omega_{\rm IR}t)\left\{\mathrm{erf}\left[\frac{(t-t_i)}{t_w}\right] - \mathrm{erf}\left[\frac{(t-t_f)}{t_w}\right]\right\}. \quad (4)$$

The IR field is smoothly turned on and off through the use of two error functions, as depicted in Fig. 1(a). $V(r)$ is the interaction of the electron with the nucleus and the core electrons (if any). For the H atom, $V(r)$ is a pure Coulomb potential, while for the He atom the following model potential is used:

$$V(r) = -0.5\frac{\alpha}{r^4}\left\{1 - \exp\left[-\left(\frac{r}{r_c}\right)^3\right]\right\}^2 - \frac{Z^*}{r}, \quad (5)$$

where $\alpha = 0.81, r_c = 1$, and $Z^* = 1 + \exp(-4.746r) + 0.2125r\exp(-3.537r)$. The model potential gives energy levels of the spin singlet of a He atom. The eigenvalues, except the ground-state energy, deviate less than 0.1% of the energy levels of a He atom. The single active electron approximation is considered in our calculation since the strengths and frequencies of the fields insures that only a single electron will participate in the dynamics.

The quantum simulation is performed by numerically solving Eq. (2). The wave function is represented on a 2D space spanned by discrete radial points and an angular momentum basis. For the radial part, a nonlinear square root mesh is used. The propagation operator is constructed using a split-operator technique of the form

$$U(\delta t) = U_1(\delta t/2)U_2(\delta t)U_1(\delta t/2), \quad (6)$$

where the approximation $U_i(\delta t) = (1 - iH_i\delta t/2)/(1 + iH_i\delta t/2)$ is used. During the time propagation, an absorbing potential is used. The radial position where the absorbing potential is turned on is set far away from the nucleus such that the potential mainly absorbs the ionized electron. One can refer to Ref. [16] for the numerical method in detail. In the following, all the data shown are collected after the IR field is smoothly turned off.

III. RESULTS AND DISCUSSION

We first discuss the results for a H atom. In order to see enough peaks in the spectrum, we choose to study the launch energy (the initial energy of electrons) ranging from $E = -0.17$ a.u. to $E = 0.11$ a.u. relative to the ionization threshold. This range covers about seven IR photons. In our simulation, the different launch energies are obtained by tuning the frequency of the UV laser. The duration of the UV laser is about four IR cycles, which is appropriate for us to see the spectrum in the energy domain (the peaks in the energy domain will be sharper for longer duration of the UV laser pulse). For each launch energy, we calculate the survival probability after the IR field is smoothly turned off, and results with six different IR intensities are compared.

In Fig. 2, the six curves correspond to the results of six different intensities, which increase from the bottom to the top. First, those curves mainly consist of a series of peaks, which are separated by the energy of one IR photon. Meanwhile, as shown in Fig. 2(a), an abnormal peak appears when the IR intensity is relatively weak. For instance, for the curve with intensity $I = 2.66 \times 10^{11}$ W/cm^2, one may expect the first left

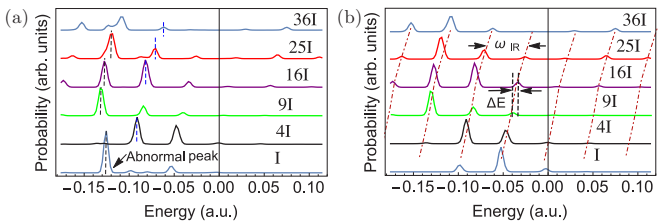

FIG. 2. (Color online) For each solid curve from the bottom to the top, IR field intensity increases from I, $4I$, $9I$, $16I$, $25I$ to $36I$. (a) Each curve records the total survival probability of H as a function of the launch energy. The vertical dotted lines help to locate the peak positions. (b) Each curve records the survival probability of H in states with principal quantum number bigger than six as a function of the launch energy. The faint (nearly vertical) lines are calculated to track the right shifting of the peaks with increasing intensities. $\triangle E$ is the difference of peak shifts for intensities $16I$ and $9I$. The periodic structure keeps the same even when we double the IR duration.

peak to sit a little left, but it is at $E = -0.125$ a.u., which is the first excited energy level of H atom. In this case, electrons with initial energy close to $E = -0.125$ a.u. will be stuck there (the $2p$ state) because the IR field intensity is too weak to trigger multiphoton transition at that binding energy. In other words, multiphoton process is a necessary condition for the formation of IR-frequency-modulated peaks. In Fig. 2(b), the abnormal peak disappears because we only count the probability of electrons bound in high-lying states. In the following section, we will see it more clearly from the probability distribution in each energy state. Second, as the field strength increases, the peaks above the ionization threshold gradually emerge, which indicates that the so-called multiphoton assisted recombination also happens in the IR field [5]. It would be interesting for experimentalists to see how far the peaks can go above the threshold if the field strength keeps increasing. Third, all the peaks tend to shift to the right with increasing intensities (the dotted nearly vertical curves make it obvious), and the shifting amount is exactly the difference of ponderomotive energy in various IR fields. Take the curves with intensity $16I$ and $9I$, for example, the amount of shifting is $\triangle E \sim 0.006$ a.u. This shift equals the difference of the ponderomotive energies of electrons when subjected to the corresponding IR fields, which is $\triangle E = F_{16I}^2/4\omega_{\mathrm{IR}}^2 - F_{9I}^2/4\omega_{\mathrm{IR}}^2$. This phenomenon can be understood if one imagines that the energy levels of high-lying states are shifted by the ponderomotive energy, thus the resonance is also shifted [17]. The peaks, respectively, are shifted by a different amount because electrons in the IR field with bigger intensity have bigger ponderomotive energy. As a final point, the periodic structure is still found when we increase the IR duration ($T_{\mathrm{IR}} = 3.2 \times 10^4$ a.u.), which is much longer than the Rydberg period ($T_{\mathrm{Ryd}} = 2\pi n^3$).

In order to understand how the electrons survive, we perform a projection of the final wave function to each bound state. By doing this, we are able to see how the survival probability is distributed in each bound state. Figures 3 and 4 show the results for different IR intensities and different initial launch energies.

The situation depicted in Fig. 3(a) is obviously different from Figs. 3(b)–3(d). The first excited state holds nearly all electrons that survive the IR field. This actually corresponds to the abnormal peak in Fig. 2(a). The launch energy is close to the first excited energy level and the IR intensity is relatively small ($I = 2.66 \times 10^{11}$ W/cm^2). The intensity is too small to trigger multiphoton absorption from the IR field, so those electrons get stuck at the first excited energy level, which is the reason why we see a big peak for $n = 2$ in Fig. 3(a). As we increase the IR intensity, the electrons cannot stay there ($n = 2$) anymore. Figures 3(b)–3(d) show the result with larger intensities, while the launch energy is still close to the first excited energy level. The probability distribution at each energy level indicates that most of the electrons that survive the IR field stay in highly excited states (principal quantum number $n \sim 10$), with binding energy ten times smaller than one IR photon. The low-lying states contribute almost nothing to the survival probability. Figure 4 gives the results for a launch energy relatively far away from the first excited state. The survival probability peaks around the same highly excited states ($n \sim 10$) for intensities $4I$, $16I$, $25I$, and $36I$, respectively. The IR duration is much longer than the Rydberg period

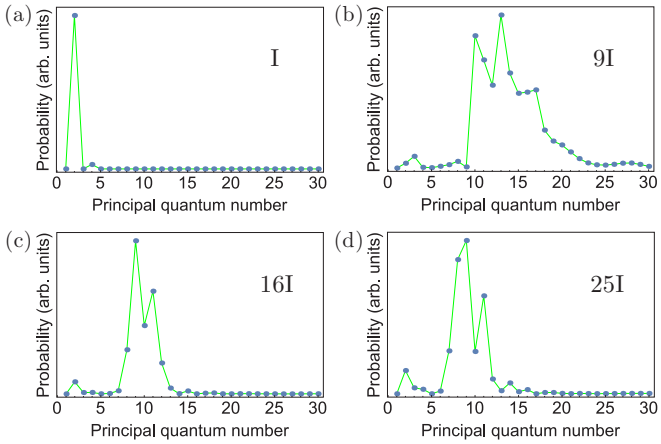

FIG. 3. (Color online) Survival probability distribution of H in each bound state for launch energy close to the first ($n = 2$) excited state. (a) IR intensity $I = 2.66 \times 10^{11}$ W/cm^2, and the initial launch energy $E = -0.125$ a.u. [marked by a vertical black line in Fig. 2(a)]. (b) IR intensity is $9I$, and $E = -0.132$ a.u. (c) IR intensity is $16I$. $E = -0.128$ a.u. (d) IR intensity is $25I$. $E = -0.120$ a.u. The energies are marked with vertical line in Fig. 2(a). For cases (b), (c), and (d), the survival probability concentrates on the highly excited states (The peak principal quantum number $n \sim 10$).

($T_{\mathrm{IR}} > T_{\mathrm{Ryd}} \sim 2\pi n^3$) of the highly excited states ($n \sim 10$), which indicates the electrons visit the core several times during the IR pulse.

Based on the above observation, the electron in highly excited states has a relatively high probability to survive, or we could say the atom becomes quasistable. In the process of time propagation, the electron can be directly excited to the quasistable states by the UV laser, or by absorbing integer

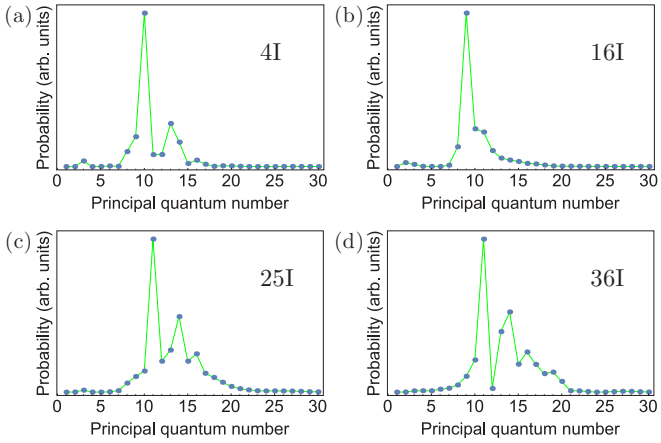

FIG. 4. (Color online) Survival probability distribution of H over each bound state for the launch energy relatively away from the first ($n = 2$) excited state. (a) IR intensity is $4I$, where $I = 2.66 \times 10^{11}$ W/cm^2, and the initial launch energy $E = -0.093$ a.u. [marked by a vertical blue line in Fig. 2(a)]. (b) IR intensity is $16I$, and $E = -0.082$ a.u. (c) IR intensity is $25I$. $E = -0.073$ a.u. (d) IR intensity is $36I$. $E = -0.0615$ a.u. The energies are marked with vertical line in Fig. 2(a). For cases (a), (b), (c), and (d), the surviving probability all closely concentrates on the relatively high excited states (peak principal quantum number $n \sim 10$).

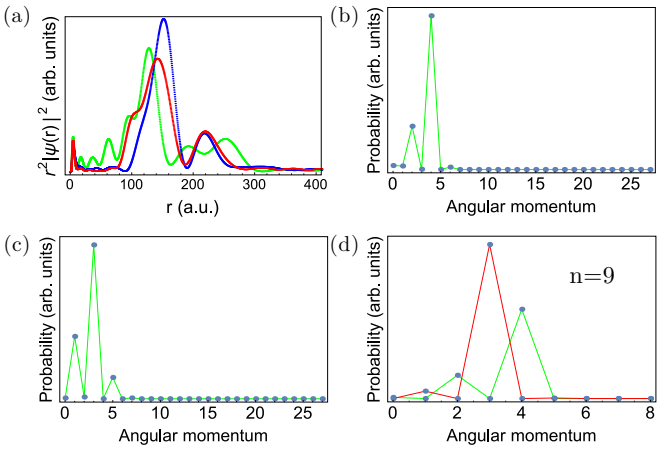

FIG. 5. (Color online) The survival probability distribution of H along the radial direction and over each orbital angular momentum. The IR intensity is $16I$, where $I = 2.66 \times 10^{11}\,\mathrm{W/cm^2}$. (a) and the launch energy is $E = -0.128$ a.u. The red, blue, and green curves correspond to the distribution at three successive times after the IR field is off. (b) The survival probability over each orbital angular momentum for launch energy $E = -0.128$ a.u. (c) The survival probability over each orbital angular momentum for launch energy $E = -0.073$ a.u. (d) The survival probability over each orbital angular momentum with $n = 9$. The green and red lines correspond to launch energy $E = -0.128$ a.u. and $E = -0.073$ a.u., respectively.

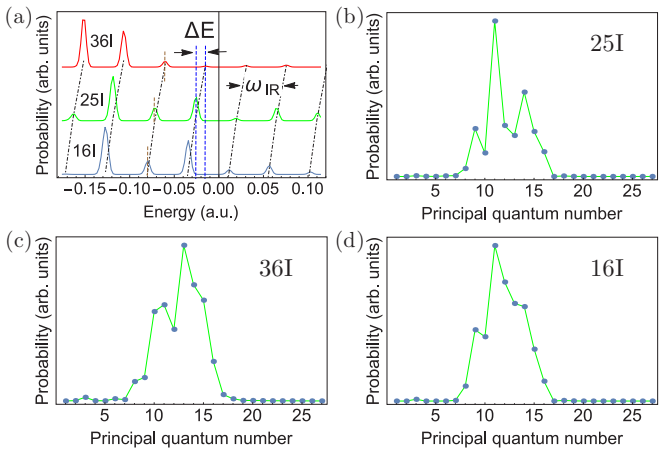

FIG. 6. (Color online) (a) Each curve records survival probability of He with principal quantum number n bigger than six. The blue, green, and red curves correspond to IR intensities $16I$, $25I$, and $36I$, respectively. The dotted (nearly vertical) curves help to track the right shifting of peaks. $\triangle E$ is the difference of peak shift for intensities $25I$ and $36I$. (b) IR intensity is $25I$, and the launch energy $E = -0.072$ a.u. [marked by a vertical brown line in panel (a)]. (c) IR intensity is $36I$, and $E = -0.063$ a.u. (d) IR intensity is $16I$, and $E = -0.082$ a.u. Panels (b), (c), and (d) give the probability distribution of He over each bound state, where electrons in the states with principal quantum number $n \sim 13$ are relatively stable.

number of IR photons after the UV laser excitation. Thus, one can imagine that electrons will have a higher probability to survive with initial energy, which allows emission or absorption of an integer number of IR photons to reach the quasistable states. These initial energies of the electrons define the positions of the peaks in Fig. 2(b). In contrast, for electrons with other initial energies, it will be relatively easy to be ionized, because they can't reach the quasistable states through multiphoton processes during the IR interaction. In short, the quasistable states act like a safe harbor, which keeps the electron bound for a relatively long time. Admittedly, the harbor is not permanently safe. The electrons in the quasistable state still have probability to be ionized, which means the peaks in Fig. 2(b) will go lower and lower with increasing IR intensity or duration.

The probability distribution along the radial direction is also checked. In Fig. 5(a), the red, blue, and green curves are picked at three successive times after the IR field is turned off. They show the radial probability distribution for IR intensity $16I$ and launch energy $E = -0.128$ a.u. Refer to the result of Fig. 3(c); the state with principal quantum number $n \sim 9$ has the biggest probability. This corresponds to the outer turning radial point 160 a.u. ($r \approx 2n^2$). As shown in Fig. 5(a), the probability is centered around $r \sim 160$ a.u. for most of the time, and the structure persists even after hundreds of IR cycles, which obviously results from the electron staying in the safe harbor (the quasistable states) in the presence of IR field. Besides, we calculate the survival probability distribution over each orbital angular momentum, as shown in Figs. 5(b) and 5(c) for launch energy $E = -0.128$ a.u. and $E = -0.073$ a.u., respectively. Figure 5(d) records the distribution with principal quantum number $n = 9$. In Fig. 5(b), the peaks at $l = 2, 4$ are due to the fact that the initial launch energy is three IR-photons away from the threshold. Thus, electrons survived at the quasistable states tend to have angular momentum $l = 0, 2, 4$ (The peak at $l = 0$ appears when using different IR intensity). The same argument applies to the result in Fig. 5(c).

In order to check that quasistability is not just for an atom with pure Coulomb potential, a simulation of He atoms is also performed. In our calculation, the single active electron approximation is used, and the electron is experiencing a model potential given by Eq. (5). The eigenenergies are obtained by numerically diagonalizing the Hamiltonian without external fields. The model potential simulates the spin singlet of a He atom. It gives a $1s^2$ state with the bound energy $E \sim -0.736$ a.u., which deviates about 0.17 a.u. from the $1s^2$ state of the He atom. For the other states, the deviation is less than 0.1%. Similar to the case of the H atom, for each launch energy we measure their survival probability, and we also perform the projection of the final wave function to the bound states. The results are shown in Fig. 6. Figure 6(a) gives the result of survival spectra for IR intensities $16I$, $25I$, and $36I$ from the bottom to the top, respectively. The IR-frequency-modulated peaks can also be seen in each curve, and as the IR intensity increases, the whole set of peaks shifts to the right, with the amount determined by the difference of electron's ponderomotive energy. Figures 6(b)–6(d) show the projection results of final wave on to the bound states, where the peaks all focus around the state with principal quantum number $n \sim 13$. These high-lying states are the quasistable states, similar to what we discussed for the case of H atoms.

IV. CONCLUSION

We have studied the quasistability of H and He atoms in the presence of an intense IR field. The survival spectra and the population distribution in each bound state reveal how electrons survive the strong IR field. In the spectra, the peaks above the threshold are due to electrons launched in the continuum. Through the process of multiphoton assisted recombination [4,5], those electrons could stimulatedly emit a certain number of IR photons, thus get caught by the core. Similar to that in the microwave experiments [2,3], the bound electron tends to stay in states with high principal quantum number, such that the electron spends a relatively long time away from the core. Instead of being ionized, electrons away from the core only experience a ponderomotive quiver motion [3,14,18]. If the electron doesn't visit the core before the laser pulse is over, it must stay bound. However, in the present case the electron does visit the core since the Rydberg period of electrons is shorter than the IR field duration ($T_{\mathrm{Ryd}} \sim 2\pi n^3 < T_{\mathrm{IR}}$). The quasistability of the states shown in Fig. 2 persists even when we double the IR duration. This indicates that atoms in quasistable states also survive collisions between the electron and the core. As a result, atoms in high-lying states become quasistable in the strong IR field. The quasistability of atoms in an IR field is essentially the same as that in a microwave field [2,3]. With the growing techniques of strong IR lasers, the phenomena discussed above could be investigated experimentally.

ACKNOWLEDGMENT

This work was supported by the U.S. Department of Energy, Office of Science, Basic Energy Sciences, under Award No. DE-SC0012193.

[1] M. W. Noel, W. M. Griffith, and T. F. Gallagher, Phys. Rev. Lett. **83**, 1747 (1999).
[2] A. Arakelyan and T. F. Gallagher, Phys Rev. A **87**, 023410 (2013)
[3] A. Arakelyan, T. Topcu, F. Robicheaux, and T. F. Gallagher, Phys. Rev. A **90**, 013413 (2014).
[4] J. H. Gurian, K. R. Overstreet, H. Maeda, and T. F. Gallagher, Phys. Rev. A **82**, 043415 (2010).
[5] E. S. Shuman, R. R. Jones, and T. F. Gallagher, Phys. Rev. Lett. **101**, 263001 (2008).
[6] W. C. Henneberger, Phys. Rev. Lett. **21**, 838 (1968).
[7] M. Pont, N. R. Walet, M. Gavrila, and C. W. McCurdy, Phys. Rev. Lett. **61**, 939 (1988).
[8] J. H. Eberly and K. C. Kulander, Science **262**, 1229 (1993).
[9] F. Benvenuto, G. Casati, and D. L. Shepelyansky, Phys. Rev. A **45**, R7670 (1992).
[10] K. C. Kulander, K. J. Schafer, and J. L. Krause, Phys. Rev. Lett. **66**, 2601 (1991).
[11] M. V. Fedorov and A. Movsesian, J. Phys. B **21**, L155 (1988).
[12] H. G. Muller, Phys. Rev. Lett. **83**, 3158 (1999).
[13] U. Eichmann, A. Saenz, S. Eilzer, T. Nubbemeyer, and W. Sandner, Phys. Rev. Lett. **110**, 203002 (2013).
[14] R. R. Jones and P. H. Bucksbaum, Phys. Rev. Lett. **67**, 3215 (1991).
[15] L. D. Noordam, H. Stapelfeldt, D. I. Duncan, and T. F. Gallagher, Phys. Rev. Lett. **68**, 1496 (1992).
[16] F. Robicheaux, J. Phys. B **45**, 135007 (2012).
[17] M. Protopapas, C. H. Keitel, and P. L. Knight, Rep. Prog. Phys. **60**, 389 (1997).
[18] R. R. Jones, D. W. Schumacher, and P. H. Bucksbaum, Phys. Rev. A **47**, R49 (1993).